Fracture-mechanics Investigations of Cracks in Rotating Disks

Aim of this work is to examine the applicability of linear-elastic fracture mechanics to a safety analysis of structural parts under centrifugal loading

by J. G. Blauel, J. Beinert and M. Wenk

ABSTRACT—Stress-intensity factors K were determined both analytically and by using a photoelastic method for the simple case of a rotating solid disk containing radial cracks. Good agreement is found not only between the calculated and the experimental K factors, but also between the static and the dynamic toughness values determined in ASTM tension tests and spin-burst tests. This confirms the applicability of linear-elastic fracture mechanics and the validity of the brittle-fracture criterion. In addition, the use of the simple superposition procedure is justified as a basis for the analysis. The possibilities of and the limitations on applying these results to practical situations are considered.

List of Symbols

a = radial position of the inner crack tip
b = radial position of the outer crack tip
d = thickness of the disk
K_I = stress-intensity factor (for mode-I-loading), $N/m^{3/2}$
K_{Ia} = stress-intensity factor at the inner crack tip
K_{Ib} = stress-intensity factor at the outer crack tip
K_{Ic} = critical stress-intensity factor for static loading in plane strain
K_{Ic}^* = critical stress-intensity factor for centrifugal loading
$l = b - a$ = crack length
N = fringe number
R = radius of the disk
r, ϕ = polar coordinates (center at middle of the disk)
S = photoelastic constant, N/fr-m
x, y = Cartesian coordinates
ν = Poisson's ratio
ρ = density
ρ, ϑ = polar coordinates (center at crack tip)
ρ_N, ϑ_N = polar coordinates of the isochromatic fringe order N
σ_1, σ_2 = principal stresses
σ_Y = material yield stress
$\sigma_y(x, 0)$ = stress distribution normal to the crack line
σ_ϕ, σ_r = principal stresses, circumferential and radial
ω = angular frequency
ω_c = critical angular frequency at failure

J. G. Blauel and J. Beinert are staff scientists, and M. Wenk is research student at the Institut für Festkörpermechanik, D-7800 Freiburg, Rosastrasse 9, Federal Republic of Germany.

Original manuscript submitted: January 2, 1976; revised version received: April 14, 1976.

Introduction and Survey

Many engineering constructions such as turbines, pumps or flywheels, involve the use of fast rotating components. To optimize their dimensions and to ensure safety in service, a precise knowledge of their strength under centrifugal loading is necessary. Conventional methods of assessment are no longer considered to be sufficient when taking into account the increasing demands for reliability of such components, their increasing size and, therefore, increasing potential risk. Recently, attempts have been made to apply the methods of fracture mechanics, which have proved successful in solving other problems of strength and safety, to this field as well (Rooke and Tweed;[1,2] Owen and Griffith;[3] ASME Safety Guide No. 14; Ricardella and Bamford[4]). These methods should provide a means of determining limiting loads for rotating parts if cracks or cracklike defects are present. In this paper (see also Wenk[5]), the applicability and the limitations of linear-elastic fracture mechanics under conditions of centrifugal loading are investigated using the simple case of a rotating solid disk. Stress-intensity factors K_I are calculated for radially oriented through-the-thickness cracks as a function of the length and the position at different angular velocities and are measured in model disks using a photoelastic method. In addition, critical stress-intensity factors K_{Ic}^* at the onset of fracture of the model disks are determined in spin-burst tests and are compared to values K_{Ic} obtained from static tension tests.

The agreement between the numerically and the experimentally determined stress-intensity factors and between the static and the dynamic critical values ($K_{Ic}^* = K_{Ic}$) confirms the applicability of linear-elastic fracture mechanics and the validity of the brittle-failure criterion that fracture takes place when $K_I \geq K_{Ic}$. In addition, the results justify the use of a simple superposition procedure to calculate stress-intensity factors as a basis for a strength analysis. The application of these results to practical situations is discussed.

The Fracture-mechanics Approach

Any fracture-mechanics safety analysis requires information from three different areas: the local stress distribution in the component (without defects) as a function of geometry and loading as well as the nature, position, shape and size of defects, and the actual material behavior in terms of a fracture-toughness parameter must be known (see, for instance, Blauel, Kalthoff, Sommer[6]).

The evaluation of the local stresses in a rotating structural part without defects is a straight-forward problem of linear elasticity, and solutions for a number of simple geometries are available in textbooks. As long as only centrifugal forces are considered, the angular frequency ω and the density ρ are the only load parameters.

In general, defects such as, for instance, inclusions, segregations, pores or cracks arising from material fabrication, production or service conditions cannot be avoided in structural members. If such defects are conservatively approximated by plane cracks (ASME BPV Code Sec. XI), their degradative influence on the structural integrity may be described in a quantitative manner by the stress-intensity factors K. These may be determined for the relevant geometry and load parameters if the rotation-induced forces are treated as static (for a constant rate of rotation) and linear-elastic material behavior is assumed. However, the analysis of the rotating part will be complex, because the finiteness of the dimensions will play an important role, because the stresses will in general vary along the length of the crack, and because mixed mode conditions will exist for all cracks which are not oriented either radially or axially.

As to the actual material behavior, experience from other types of strength problems and with different materials leads one to expect that a failure criterion $K_I \geqq K_{Ic}$* can also be applied under conditions of centrifugal loading. Accordingly, an existing crack in a rotating disk will start to extend in a brittle way if the stress-intensity factor K_I—for an assumed opening mode of loading on the crack—becomes equal to or exceeds a critical threshold value, the fracture toughness K_{Ic}*. This is a material constant defining a minimum resistance to fracture propagation and which can be determined independently by laboratory tests. A comparison of the limiting loads in spin-burst tests with conventional tension tests should prove the validity of this criterion and provide a sound basis for its applicability to a strength and safety analysis in practical situations.

Analytical Determination of Stress-intensity Factors

The type of specimen chosen as an example for this investigation was a disk of constant thickness without a central hole. The geometry, coordinates and other parameters are shown in Fig. 1.

When rotating at a constant angular frequency ω, stresses σ_ϕ and σ_r are generated which are oriented in circumferential and radial direction; σ_ϕ and σ_r are principal stresses and can be assumed constant through the thickness for $d << R$ (Timoshenko and Goodier[7]):

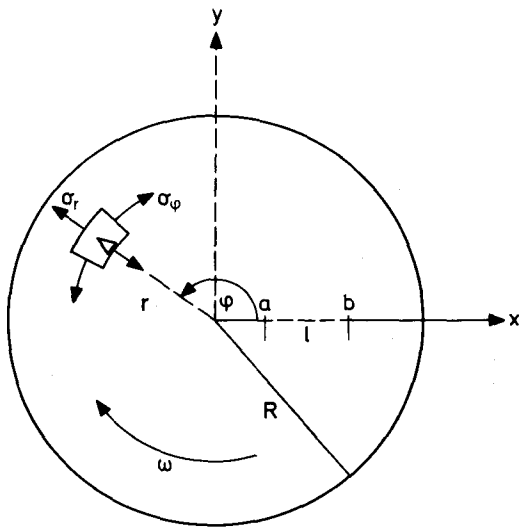

R = external radius; d = thickness with d/R << 1; x, y = Cartesian coordinates; r, ϕ = polar coordinates; a, b = tips of a radially oriented through-the-thickness crack; b − a = l = crack length; ω = angular frequency; σ_r, σ_ϕ = radial and circumferential stresses

Fig. 1—Geometry, coordinates and other parameters of the rotating disk

$$\sigma_\phi(r) = \rho\omega^2 \left\{ \frac{3+\nu}{8} R^2 - \frac{1+3\nu}{8} r^2 \right\}$$

$$\sigma_r(r) = \rho\omega^2 \frac{3+\nu}{8} \{R^2 - r^2\} \qquad (1)$$

Here, density ρ and Poisson's ratio ν are the only material constants. Figure 2 shows a numerical evaluation of eq (1) for the geometry and material conditions of the model experiments described in the following section.

As the most critical situation in a structural member (and which can be most easily analyzed), radially oriented through-the-thickness cracks were investigated. The loading by the circumferential stresses $\sigma_\phi(r)$ is, then, of the simple mode I type but it varies along the crack length l and is, in general, unsymmetric about the crack center. Here, the method of superposition can be used to evaluate stress-intensity factors. For the general situation sketched in Fig. 3, one obtains following Paris and Sih[8]:

$$K_{Ia} = \sqrt{\frac{2}{\pi(b-a)}} \int_a^b \sigma_y(x,0) \sqrt{\frac{b-x}{x-a}}\, dx$$

$$K_{Ib} = \sqrt{\frac{2}{\pi(b-a)}} \int_a^b \sigma_y(x,0) \sqrt{\frac{x-a}{b-x}}\, dx \qquad (2)$$

where K_{Ia} and K_{Ib} are the stress-intensity factors for the crack with one tip at $x = a$ and the other at $x = b$ and $\sigma_y(x,0)$ is the stress distribution along the crack line calculated from the external loading but for the

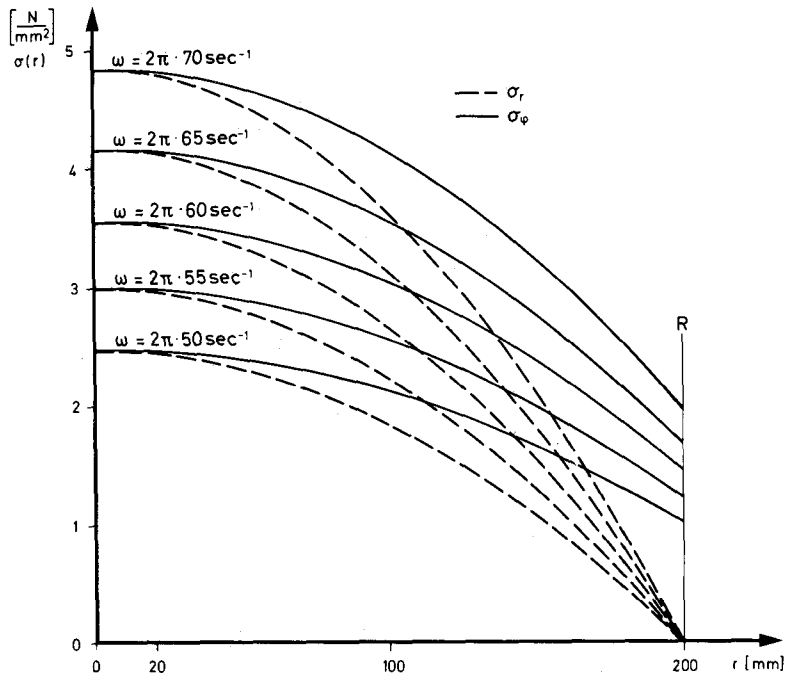

Material: $\rho = 1.5 \cdot 10^3$ kg/m³, $\nu = 0.33$ (PMMA or ARALDIT B)

Fig. 2—Radial σ_r and circumferential stresses σ_ϕ in a rotating disk

crack-free body. For the rotating disk, x has to be replaced by r and $\sigma_y(x, 0)$ by $\sigma_\phi(r)$ according to eq (1):

$$K_{Ia} = \frac{\sqrt{2}}{8\sqrt{\pi(b-a)}} \rho\omega^2 \int_a^b \{(3+\nu)R^2 - (1+3\nu)r^2\} \sqrt{\frac{b-r}{r-a}}\, dr$$

$$K_{Ib} = \frac{\sqrt{2}}{8\sqrt{\pi(b-a)}} \rho\omega^2 \int_a^b \{(3+\nu)R^2 - (1+3\nu)r^2\} \sqrt{\frac{r-a}{b-r}}\, dr \qquad (3)$$

In the same way as the stresses, the stress-intensity factors depend linearly on the density ρ and are proportional to the square of the angular frequency ω; Poisson's ratio ν comes into the picture in a more complicated way. Basically, the stress-intensity factors at the two tips of all unsymmetrical cracks are different, with $K_{Ia} \geqq K_{Ib}$; only in the central regions $|r| < 0.2R$ they are more or less equal because the stresses are nearly equal. The actual values will depend on the crack length and the locus of the crack center. Equation (3) has been evaluated numerically and results are shown in Figs. 8, 9 and 10.

The assumption of an infinite region for the derivation of eqs (2) and (3) seems to exclude their applicability for situations where either the crack length is not small compared to the radius of the disk or one of the crack tips is near to the periphery. This would be a consequence of the additional moments induced by the opening crack. But comparing this situation with that of a finite-width plate with an edge crack under tension, an appreciable reduction of this effect can be expected in the case of the rotating disk due to the higher degree of connectivity. A quantitative measure of this is obtained by comparing our results with those derived from the complete solution of Rooke and Tweed[1] for the finite-width disk. As Fig. 4 shows, there is only a difference of less than 8 percent for cracks within 80 percent of the disk radius; the deviation was found to be of the same sense and of the same magnitude for other crack configurations. For very long cracks or edge cracks, no results of Rooke and Tweed[1,2] are available. In the comparison with the experimentally determined

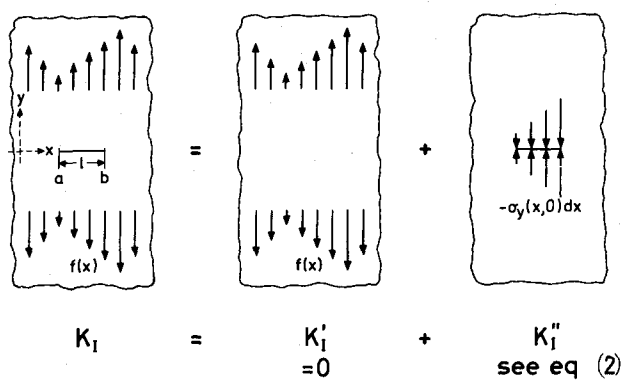

f(x) – given distribution of external forces. $\sigma_y(x, 0)$ = distribution of stresses in the crack-free body induced by the external forces f(x) along the prospective crack-line; $-\sigma_y(x, 0)$ = distribution of forces acting along the crack line to induce stress-free boundaries by superposition to the forces due to the stresses $\sigma_y(x, 0)$

Fig. 3—Principle of the method of superposition

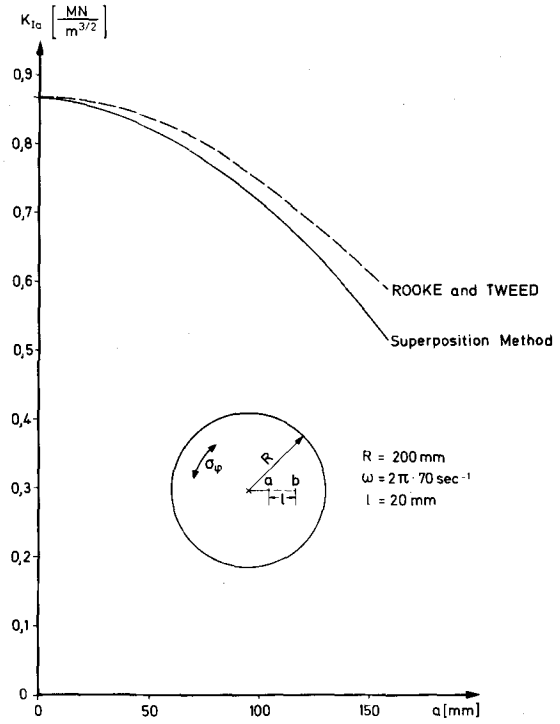

Stress-intensity factor K_{Ia} for the inner tip of a radial crack in a disk ($\rho = 1.5 \cdot 10^3$ kg/m³, $\nu = 0.33$) under centrifugal loading

Fig. 4—Comparison of results from the superposition method and the solution of Rooke and Tweed[1]

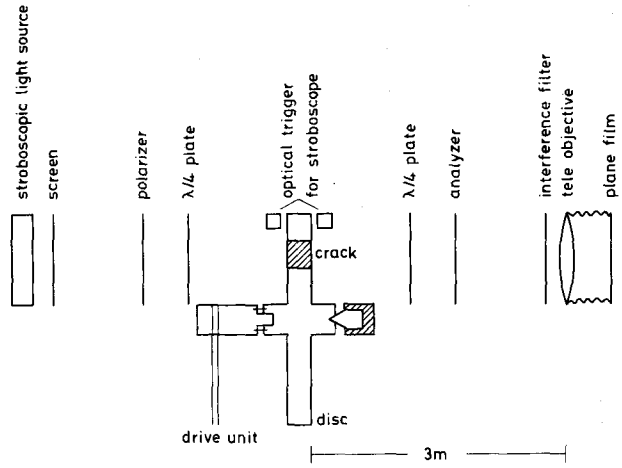

Fig. 5—Schematic sketch of the arrangement for the photoelastic determination of stress-intensity factors in a rotating cracked disk

stress-intensity factors in the next section, only the superposition-method results are used.

Experimental Determination of Stress-intensity Factors

To check the analytical results of the preceding section, small-scale precracked models made from a suitable transparent material were used. The stress-intensity factors under rotation were determined using a photoelastic procedure with stroboscopic illumination. Figure 5 shows the *experimental arrangement* schematically. The disk was held between a point bearing and a trunnion seat both acting on bosses glued to the disk surfaces and it was driven by an infinitely variable electric motor. An opaque marker near the periphery of the disk was used both to determine the rotation frequency and to trigger the light source (Stroboscope Philips PR 9107) through interruption of a light-beam incident for the photoelastic system. The other components of the photoelastic system were two polarizing filters with quarter-wave plates, an interference filter for monochromatic light and a camera with a long-focal-length objective (Leitz Telyt 1:5, f = 400 mm) to approximate to parallel-light illumination. Figure 6 shows a series of photoelastic pictures of a crack in a disk rotating at different speeds taken with the above arrangement.

The *model disks* were made from plates of ARALDIT B (Firma Tiedemann, Garmisch-Partenkirchen), a material with a small photoelastic constant ($S = 10.2 \cdot 10^3$ N/fr-m) and approximating closely to linear-elastic fracture behavior. The diameter of the disks was $2R = 400$ mm and their thickness $d = 10$ mm. The artificial cracks were saw cuts (0.2-0.4 mm wide) which were sharpened with a razor blade.

The *evaluation* of the fringe pattern at the crack tip relies on the validity of the so-called basic equation of photoelasticity and the linear-elastic crack-tip stress-field equations. The first of these

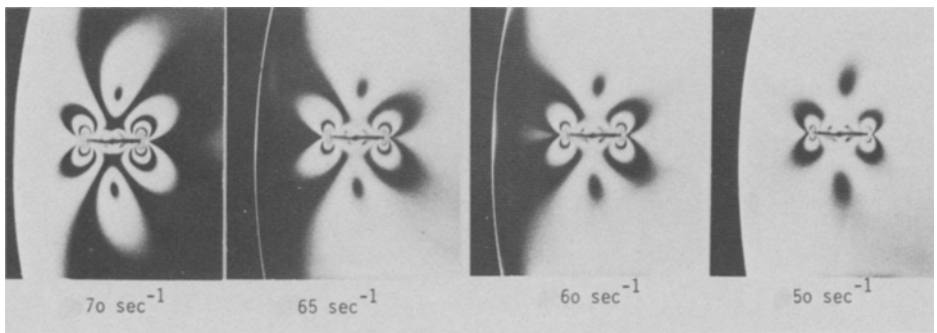

Material: ARALDIT B; d = 10 mm, R = 200 mm, l = 13 mm, a = 162.5 mm

Fig. 6—Isochromatic-fringe patterns of a crack in a rotating disk at different angular frequencies

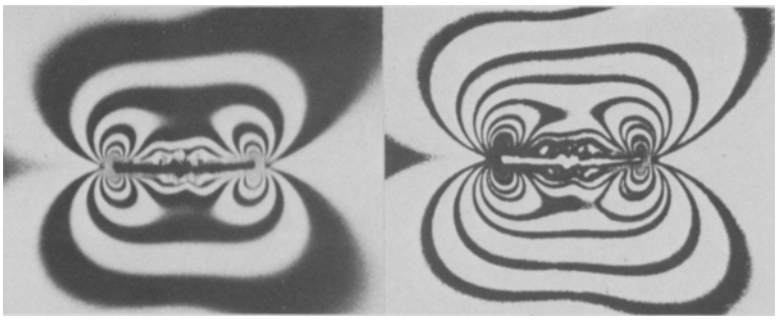

Disk: ARALDIT B, R = 200 mm, d = 10 mm, crack: a = 100 mm, l = 15 mm, $\omega = 2\pi 65\ s^{-1}$

Fig. 7—Isochromatic fringes around a radial crack in a rotating disk together with the corresponding patterns of equal-density contours

$$N = \frac{\Delta s}{\lambda} = \frac{d}{S}(\sigma_1 - \sigma_2) \tag{4}$$

gives a linear relationship between the fringe number N—which is the change of optical path-length Δs due to the stresses divided by the wavelength λ of the light—and the principal-stress difference $\sigma_1 - \sigma_2$ in the loaded specimen; with the photoelastic constant S being the stresses in N/mm² required to produce the first isochromatic fringe in a specimen of thickness $d = 1$ mm. The second equation

$$\sigma_1 - \sigma_2 = \left[\frac{K_I}{4} \sin^2\vartheta - \frac{K_I}{\sqrt{2\pi\rho}} 8a_2 \sin\vartheta \sin\frac{3}{2}\vartheta \right]^{1/2} \tag{5}$$

includes the first terms of a general series-representation in polar coordinates ρ, ϑ of the stresses in the neighborhood of a crack tip under a pure mode I loading according to Irwin.[9] The stress-intensity factor K_I and the coefficient a_2 are determined by the boundary conditions of geometry and load. They can be evaluated experimentally by comparing the theoretical lines of constant principal-stress difference according to eq (5) with the isochromatics described by eq (4). This fit was accomplished by a numerical regression program of Klein.[10] Any one of the isochromatics can be used for such a determination provided that it is not disturbed by the boundary of the disk so that eq (5) can be applied. For the fitting program, it is important to measure very precisely the coordinates ρ_N and ϑ_N along the isochromatic of order N, which is usually a relatively wide fringe. Therefore, all negatives of fringe patterns were recopied onto an equal-density film (Agfa Contour) which gives two narrow lines from contours of equal density which are symmetrical about the center of an isochromatic fringe. These can then be localized very precisely using a microscope. An example is shown in Fig. 7.

The *results* of the measurements are shown in Figs. 8, 9 and 10. There, the experimentally determined stress-intensity factors K_I for different crack lengths, crack positions and angular frequencies of the model disks are compared with theoretical values from eq (3). For the experimental values, the standard deviation is shown which reflects the uncertainties in measuring crack length, coordinates ρ_N and ϑ_N, and photoelastic constant S and the error from the numerical procedure.

Within the accuracy of the measurements, the experimental and theoretical values are in good agreement. The three series of results show that the stress-intensity factor at the inner crack tip (as a consequence of the stress distribution) is always greater than at the outer one. Therefore, onset of the unstable crack extension can always be expected to occur at the inner crack tip.

Figure 8 confirms the dependence of K_I on the square of the angular frequency ω. In the lower part of the curve, an exact experimental evaluation is no longer possible because the number of fringes is too small.

In the test series of Fig. 9, the locus of the outer crack tip had been held constant but the crack length varied. For increasing crack length, the risk of unstable fracture also increases and the difference between K_{Ia} and K_{Ib} gets larger. If the position of a crack is varied (see Fig. 10) at a constant crack length and a constant angular velocity, the stress-intensity factors decrease with increasing distance from the center of the disk. In the central part of the disk ($|r| < 0.2R$) the stress-intensity factors tend towards a constant maximum value.

Spin-burst Tests and the Brittle-failure Criterion

To verify the brittle-failure criterion that fracture will take place when $K_I \geqq K_{Ic}$, a series of cracked model disks was loaded to fracture in spin-burst tests. From the limiting angular frequency and the relevant geometrical data of disk and crack a critical stress-intensity factor K_{Ic}^* was determined following eq (3) (using the expression for K_{Ia} since $K_{Ia} \geqq K_{Ib}$). Single-edge-notched specimens were machined afterwards from the broken parts of the disks and were tested according to the recommendations of fracture toughness K_{Ic} determination (ASTM—Designation E 399-72). Table 1 compares the results of seven series of tests on ARALDIT B and PMMA specimens.

Taking into account the limited number of tests and the uncertainties of measurement, these results show that, in the spin-burst tests, fracture is initiated for all crack positions and crack lengths at a constant material specific value K_{Ic}^* of the stress-intensity factor. In addition, Table 1 shows that K_{Ic}^* is equal to the statically determined value K_{Ic}. Therefore, it can be concluded that, for conditions of centrifugal loading, onset of brittle fracture is also determined by the fracture toughness K_{Ic}.

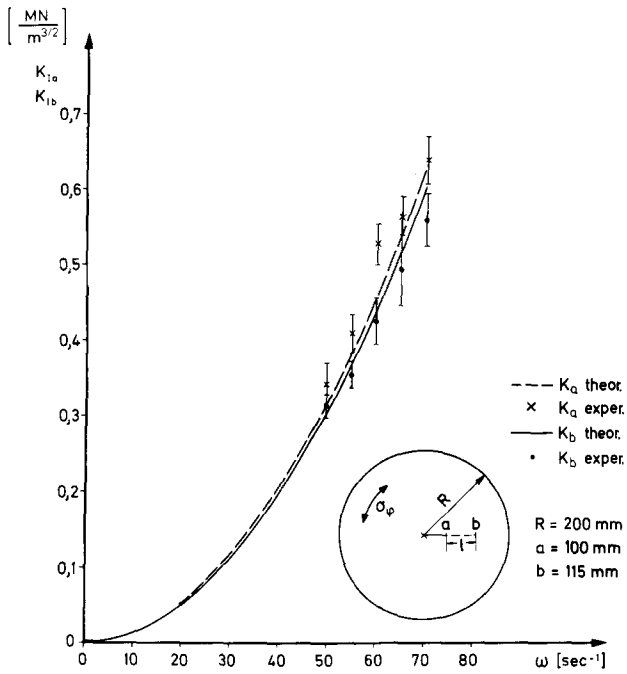

(R = 200 mm, $\rho = 1.5 \cdot 10^3$ kg/m³, $\nu = 0.33$) as a function of angular frequency

Fig. 8—Measured and calculated stress-intensity factors K_I for a crack of length $l = 15$ mm in a rotating disk of ARALDIT B

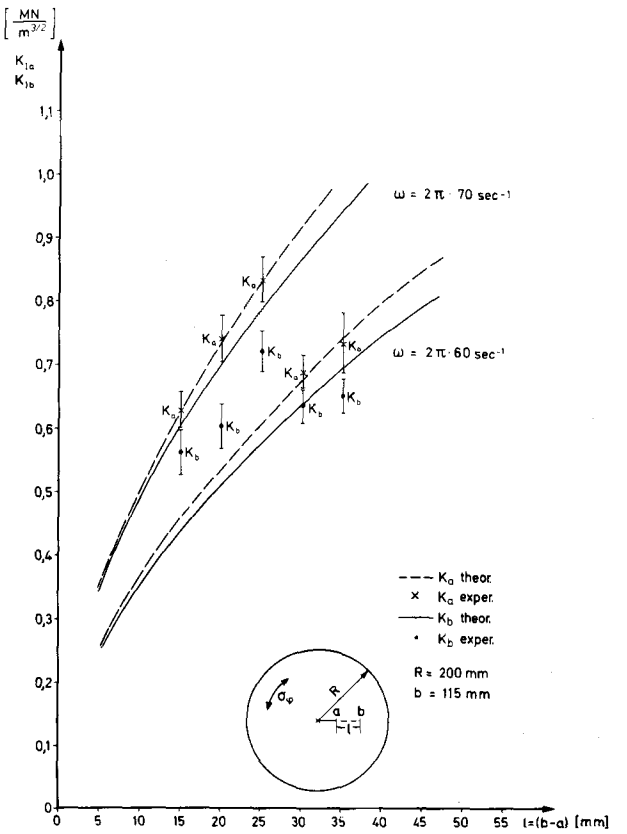

Material: ARALDIT B

Fig 9—Measured and calculated stress-intensity factors for 5 different crack lengths $l = b - a$ at two different angular velocities ω

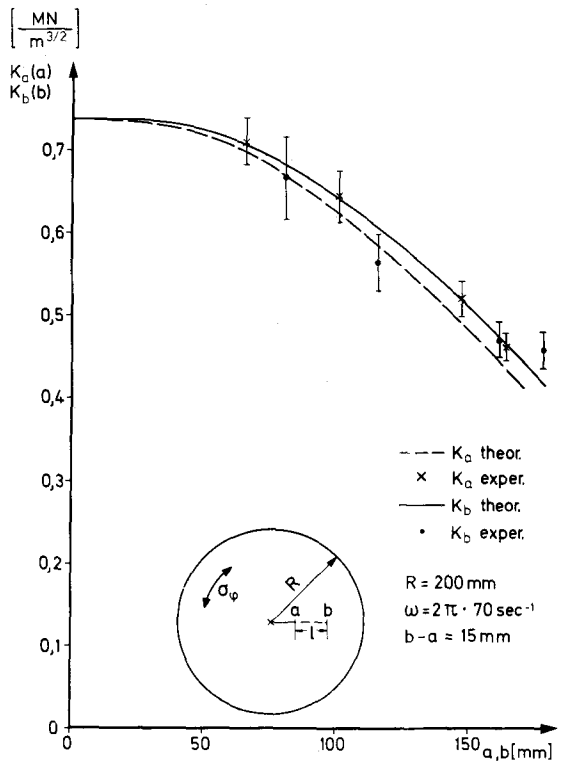

Dashed line: $K_a = K_a$ (a) Full line: $K_b = K_b$ (b)
(Note: for one value of the a, b axis, the two curves describe two different crack configurations)
Material: ARALDIT B

Fig. 10—Measured and calculated stress-intensity factors for cracks of constant length $l = b - a$ at different positions in the disk

Consequences for a Strength and Failure Analysis

The model experiments using cracked disks of PMMA and ARALDIT B confirm the applicability of the analytical and experimental methods of linear-

TABLE 1—COMPARISON OF CRITICAL STRESS-INTENSITY FACTORS K_{Ic}* AND K_{Ic} FOR ARALDIT B AND PMMA†

Material	Radial a mm	Crack l mm	'Dynamic' Test ω_{crit} s^{-1}	'Dynamic' Test K_{Ic}* MN/m$^{3/2}$	'Static' Test K_{Ic} MN/m$^{3/2}$
Araldit B	100	15	$77 \cdot 2\pi$	0.775 (5)	
Araldit B	90	25	$72 \cdot 2\pi$	0.866 (5)	0.79 ± 0.2 (20)
Araldit B	80	35	$65 \cdot 2\pi$	0.863 (5)	
		mean value		0.83 ± 0.13	
PMMA	60	20	$97 \cdot 2\pi$	1.236 (5)	
PMMA	90	20	$103 \cdot 2\pi$	1.316 (5)	1.45 ± 0.38 (10)
PMMA	110	20	$112 \cdot 2\pi$	1.404 (5)	
PMMA	130	20	$119 \cdot 2\pi$	1.445 (5)	
		mean value		1.36 ± 0.32	

† Determined in spin-burst tests using eq (3) and by conventional fracture-toughness tests under pure static tension (the numbers in brackets are the numbers of tests; specimen thickness in all cases d = 10 mm).

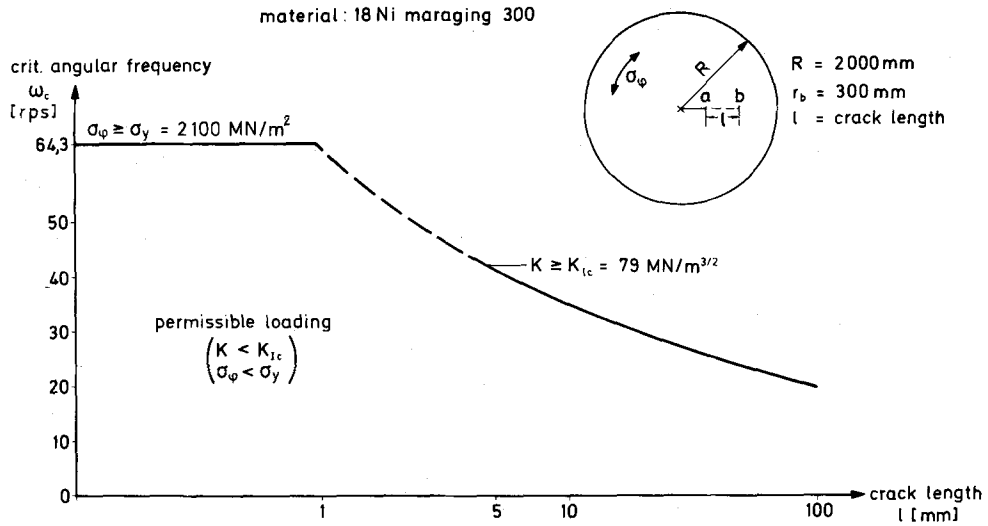

Fig. 11—Maximum allowable angular frequencies ω_c for an energy-storage flywheel made of 18 Ni maraging steel grade 300 as a function of crack length l

elastic fracture mechanics for centrifugal loading. Therefore, if the same general conditions of material behavior, existence of cracklike defects and state of stress (see second section) are given, these results can be used to analyze real technical situations (see Greenberg et al.[11]). In the following, as an example, the results of the preceding sections are used to determine the limiting loading of an energy-storage flywheel made of steel.

The storage wheel is assumed to be a solid disk of radius $R = 2000$ mm made of high-strength maraging steel (X2 Ni Co Mo 18 9 5 $\hat{=}$ 18 Ni grade 300). To obtain a safe limit, the worst assumptions are made for possible defects in the disk: cracks exist in the central region which go through the full thickness and are radially oriented. Using the simplified version of eq (3) for $|r| < 0.2R$

$$K_{Ia} \approx K_{Ib} \approx \frac{3+\nu}{8} R^2 \rho \omega^2 \sqrt{\pi \frac{l}{2}} \qquad (6)$$

and the brittle-failure criterion together with the material values

$$\rho = 7.85 \cdot 10^3 \frac{\text{kg}}{\text{m}^3} \qquad \nu = 0.3, \qquad K_{Ic} = 79\ \text{MN/m}^{3/2}$$

the maximum allowable angular frequencies

$$\omega_c = \frac{2}{R} \sqrt{\frac{2K_{Ic}}{\rho(3+\nu)\sqrt{\pi\, l/2}}} \qquad (7)$$

are calculated. These are plotted in Fig. 11 as a function of crack length l.

The linear-elastic fracture-mechanics approach, i.e., eq (7), is no longer valid if the material yield stress σ_Y is exceeded in larger areas of the disk. Then the disk will fail by plastic collapse independently of crack length at a critical angular frequency

$$\omega_c = \frac{2}{R} \sqrt{\frac{2\sigma_Y}{\rho(3+\nu)}} \qquad (8)$$

This limit is also shown in Fig. 11. Thus the maximum allowable angular frequency is determined by either eq (7) or eq (8), depending on which one gives the smaller value of ω_c. This, in turn, determines the maximum amount of kinetic energy

$$E_{\max} = \frac{1}{4} \pi \cdot R^4 \cdot d \cdot \rho \cdot \omega_c^2 \qquad (9)$$

which can be stored in such a disk.

Acknowledgment

The work on which this publication is based formed part of an investigation by the firm of Maschinenfabrik Augsburg-Nürnberg (MAN) into the possible use of flywheels for energy storage. This investigation was funded by the Bundesminister für Forschung und Technologie (BMFT) of the Federal Republic of Germany. The BMFT accepts no responsibility for the correctness, accuracy and completeness of this work nor any liability for the rights of third parties.

References

1. *Rooke, D. P. and Tweed, J., "The Stress Intensity Factors of a Radial Crack in a Finite Rotating Elastic Disc," Intnl. J. Engrg. Sci., 10, 323-335 (1972).*
2. *Rooke, D. P. and Tweed, J., "The Stress Intensity Factor of an Edge Crack in a Finite Rotating Elastic Disc," Intnl. J. Engrg. Sci., 11, 279-283 (1973).*
3. *Owen, D. R. J. and Griffiths, J. R., "Stress Intensity Factors of Cracks in a Plate Containing a Hole and in a Spinning Disc," Intnl. J. of Fract., 9 (4), 471-476 (1973).*
4. *Ricardella, P. C. and Bamford, E. H., "Reactor Coolant Pump Flywheel Overspeed Evaluation," ASME 74-PVP-25 (1974).*
5. *Wenk, M., "Bruchmechanische Untersuchungen zum Festigkeitsverhalten von rissbehafteten rotierenden Scheiben," Diploma-Thesis, Univ. Freiburg, (Germany) (1975).*
6. *Blauel, J. G., Kalthoff, J. F. and Sommer, E., "Die Bruchmechanik als Grundlage für das Verständnis des Festigkeitsverhaltens," Materialprüfung, 12 (3), 69-76 (1970).*
7. *Timoshenko, J. and Goodier, J. N., Theory of Elasticity, McGraw-Hill Inc., New York, NY (1965).*
8. *Paris, P. C. and Sih, G. C., "Stress Analysis of Cracks," ASTM Spec. Tech. Pub. (381), 30-83 (1965).*
9. *Irwin, G. R., Disc. on paper by Wells, A. A. and Post, D., "The Dynamic Stress Distribution Surrounding a Running Crack—A Photoelastic Analysis," Proc. of the SESA, 16 (1), 93-96 (1958).*
10. *Klein, G., "Bestimmung von Spannungsfaktoren bei gemischten Beanspruchungsarten am Beispiel eines Risses in der Umgebung eines Kreislochs," Dissertation Karlsruhe (Germany) (1974).*
11. *Greenberg, H. D., Wessel, E. T. and Pryle, W. H., "Fracture Toughness of Turbine Generator Rotor Forgings," Engrg. Fract. Mech., 1, 653-674 (1970).*